Breakdown of the Kohn theorem near a Feshbach resonance in a magnetic trap

Hamid Al-Jibbouri[1,*] and Axel Pelster[2,3,†]

[1]*Institut für Theoretische Physik, Freie Universität Berlin, Arnimallee 14, 14195 Berlin, Germany*
[2]*Fachbereich Physik und Forschungszentrum OPTIMAS, Technische Universität Kaiserslautern, 67663 Kaiserslautern, Germany*
[3]*Hanse-Wissenschaftskolleg, Lehmkuhlenbusch 4, D-27733 Delmenhorst, Germany*

We study the collective excitation frequencies of a harmonically trapped ^{85}Rb Bose-Einstein condensate (BEC) in the vicinity of a Feshbach resonance. To this end, we solve the underlying Gross-Pitaevskii (GP) equation by using a Gaussian variational approach and obtain the coupled set of ordinary differential equations for the widths and the center of mass of the condensate. A linearization shows that the dipole-mode frequency decreases when the bias magnetic field approaches the Feshbach resonance, so the Kohn theorem is violated.

I. INTRODUCTION

Many experiments focus on investigating collective excitations of harmonically trapped Bose-Einstein condensates (BECs) because they can be measured very accurately and, therefore, allow for extracting the respective system parameters [1]. Several studies show that the excitation of low-lying collective modes can be achieved by modulating a system parameter. One example is to change periodically the external potential trap [2–8] or, more specifically, the trap anisotropy of the confining potential [5,9–13]. Alternatively, this can also be achieved by a periodic modulation of the *s*-wave scattering length [14–20] or, possibly, by modifying the three-body interaction strength [12,13,18].

In 1961 Kohn [21] showed in a three-dimensional solid that the Coulomb interaction between electrons does not change the cyclotron resonance frequency. This Kohn theorem can also be transferred to the realm of ultracold quantum gases, where it states that the center of mass of the entire cloud oscillates back and forth in the harmonic trapping potential with the natural frequency of the trap irrespective of both the strength and type of the two-body interaction. The Kohn theorem for a Bose gas is discussed explicitly in the Bogoliubov approximation at zero temperature of Ref. [22]. The dynamics of a trapped Bose-condensed gas at finite temperature is consistent with a generalized Kohn theorem and satisfies the linearized Zaremba-Nikuni-Griffin (ZNG) hydrodynamic equations in Ref. [23]. In particular, the Kohn mode was studied in an approximate variational approach to the kinetic theory in the collisionless regime in Ref. [24]. The validity of the Kohn theorem at finite temperature was also shown within a linear response treatment in Ref. [25]. Later on it was also examined in Ref. [26] for a specific finite-temperature approximation within the dielectric formalism. Furthermore, the dipole-mode frequency was studied by using a sum-rule approach in Refs. [27–31]. The collective dipole oscillations in the Bose-Fermi mixture were studied theoretically in Refs. [28,29] and experimentally in Ref. [32], while the dipole oscillation of a spin-orbit-coupled Bose-Einstein condensate

confined in a harmonic trap was studied experimentally [30] and investigated theoretically [30,31]. The dipole oscillation was also discussed for a general fermionic mixture by using the Boltzmann equation in Ref. [33].

Apart from a periodic modulation of a system parameter the dipole mode can also be excited by introducing an abrupt change in the potential. The experimental achievement [1,34] has been confirmed in Refs. [35,36], where also the quadrupole frequency was determined as an eigenfrequency of the hydrodynamic equations. The coupling between the internal and the external dynamics of a Bose-Einstein condensate oscillating in an anharmonic magnetic waveguide was studied in Ref. [37]. There are also several nonlinear effects including second- and third-harmonic generation of the center-of-mass motion, and a nonlinear mode mixing has been identified. In the more recent work [38], the authors explored a different physical idea by investigating the coupling between dipole and quadrupole modes in the immediate vicinity of a Feshbach resonance. They started by considering a Bose-Einstein condensate in a magneto-optical Ioffe-Pritchard trap [39] with a controlled bias field, where the dipole mode is excited. If the bias field is close enough to a Feshbach resonance, the oscillation of the entire cloud through the inhomogeneous bottom of the trap causes an effective periodic time-dependent modulation in the scattering length, which in turn changes the Kohn mode frequency but also excites other modes like the quadrupole or the breathing mode.

Although Ref. [38] introduces this appealing physical notion, it only provides a rough quantitative study. Therefore we calculate in this paper in detail the collective excitation modes of a harmonically trapped Bose-Einstein condensate in the vicinity of a Feshbach resonance for experimentally realistic parameters of a ^{85}Rb BEC [40,41]. To this end, we consider the situation that a Bose-Einstein condensate oscillates within a dipole mode in the *z* direction and investigate how the dipole-mode frequency changes when the bias magnetic field approaches the Feshbach resonance in Sec. II. Afterwards, we follow Ref. [38] and transform the partial differential of the GP equation [42,43] for the condensate wave function in Sec. III within a variational approach [44,45] into a set of ordinary differential equations for the widths and the center-of-mass position of the condensate in an axially symmetric harmonic trap plus a bias potential. Our

*hamidj@fu-berlin.de
†axel.pelster@physik.uni-kl.de

analysis is based on an exact treatment with the help of the Schwinger trick [46]. The resulting theory on how to determine the low-lying collective excitation frequencies is developed step by step in Sec. IV. Afterwards, Sec. V compares our results with the corresponding findings of Ref. [38]. In addition we discuss two special cases, when the bias magnetic field field approaches the Feshbach resonance and when it is far away from the Feshbach resonance. It turns out that the heuristic approximation in Ref. [38] is not valid neither on top of the Feshbach resonance, nor far away from it. Finally, in Sec. VI we summarize our findings and present the conclusions.

II. NEAR FESHBACH RESONANCE

The dynamics of a condensed Bose gas in a trap at zero temperature is described by the time-dependent GP equation [44,45]

$$i\hbar \frac{\partial \psi(\mathbf{r},t)}{\partial t} = \left[-\frac{\hbar^2}{2M} \Delta + V_{\text{ext}}(\mathbf{r}) + g_2 N n_c(\mathbf{r},t) \right] \psi(\mathbf{r},t), \quad (1)$$

where $\psi(\mathbf{r},t)$ denotes a condensate wave function and N represents to the total number of atoms in the condensate. On the right-hand side of the above equation we have a kinetic-energy term, where M denotes the mass of the corresponding atomic species, an external trap $V_{\text{ext}}(\mathbf{r})$, and the third term is the two-body interaction with the condensate density $n_c(\mathbf{r},t) = |\psi(\mathbf{r},t)|^2$ and the strength $g_2 = 4\pi\hbar^2 a_s/M$, which is proportional to the s-wave scattering length a_s. In the presence of a magnetic field, the s-wave scattering length can be tuned by applying an external magnetic field due to the Feshbach resonance [35,47]:

$$a_s(B) = a_{\text{BG}}\left(1 - \frac{\Delta}{B - B_{\text{res}}}\right), \quad (2)$$

with the background s-wave scattering a_{BG}, the width of the Feshbach resonance Δ, and the resonance of magnetic field B_{res}. In this paper, we consider a Bose-Einstein condensate confined in a magneto-optical Ioffe-Pritchard trap composed of a cylindrically symmetric harmonic potential with trap anisotropy λ plus a bias [38,39]:

$$V_{\text{ext}}(\mathbf{r}) = V_0 + \frac{M\omega_\rho^2}{2}(\rho^2 + \lambda^2 z^2). \quad (3)$$

Due to the atomic magnetic moment μ_B the potential is generated by a corresponding magnetic field whose modulus is given by

$$B = B_0 + \frac{M\omega_\rho^2}{2\mu_B}(\rho^2 + \lambda^2 z^2), \quad (4)$$

where $B_0 = V_0/\mu_B$ is the bias field.

From Eqs. (2) and (4), the interparticle interaction in the atomic cloud moving in this potential is controlled by the spatially dependent scattering length

$$a_s = a_{\text{BG}}\left[1 - \frac{\Delta}{\mathcal{H} + \frac{M\omega_\rho^2}{2\mu_B}(\rho^2 + \lambda^2 z^2)}\right], \quad (5)$$

where $\mathcal{H} = B_0 - B_{\text{res}}$ denotes the deviation of the bias magnetic field B_0 from the location of the Feshbach resonance at B_{res}. In the following, we consider the potential (3) loaded with a condensed cloud whose dipole mode is excited in the z direction. In this configuration, far away from the Feshbach resonance, the center of mass oscillates periodically at the bottom of the trap with the Kohn mode frequency $\omega_z = \lambda\omega_\rho$.

As an initial physical motivation we discuss the consequences of the Thomas-Fermi (TF) approximation. Because we assume to have a strong two-body interaction, we neglect the kinetic-energy term in the time-independent counterpart of Eq. (1) and obtain

$$\mu = V_{\text{ext}}(\mathbf{r}) + g_2 n_c(\mathbf{r}). \quad (6)$$

Far away from the Feshbach resonance we can consider the potential contribution in Eq. (5) to be small, thus we expand Eq. (5) up to the first order of the external potential, yielding

$$\mu = V_{\text{ext}}(\mathbf{r}) + \frac{4\pi\hbar^2 a_{\text{BG}} n_c(\mathbf{0})}{M}$$
$$\times \left[1 - \frac{\Delta}{\mathcal{H}} + \frac{\Delta M\omega_\rho^2}{2\mathcal{H}^2\mu_B}(\rho^2 + \lambda^2 z^2) + \cdots\right], \quad (7)$$

where $n_c(\mathbf{0})$ is the TF density at the trap center with the chemical potential $\mu = (\hbar\omega_\rho/2)(15N\lambda a_{\text{eff}}/l)^{2/5}$. On the one hand we read off from Eq. (7) an effective s-wave scattering length

$$a_{\text{eff}} = a_{\text{BG}}\left(1 - \frac{\Delta}{\mathcal{H}}\right). \quad (8)$$

In the following discussion we have a ^{85}Rb BEC in mind, whose Feshbach resonance is characterized by a negative background value of the s-wave scattering length, i.e., $a_{\text{BG}} < 0$, and a positive width, i.e., $\Delta > 0$ [40,41]. Thus, the BEC is unstable, i.e., $a_{\text{eff}} < 0$, provided that $B_0 < B_{\text{crit}} + \Delta$. Conversely, the TF approximation yields a stable BEC, i.e., $a_{\text{eff}} > 0$, in the case that $B_{\text{res}} < B_0 < B_{\text{crit}} = B_{\text{res}} + \Delta$. On the other hand, we obtain from Eqs. (3) and (7) an effective Kohn mode frequency

$$\omega_{D,\text{eff}} = \lambda\omega_\rho \sqrt{1 + \frac{4\pi\hbar^2 a_{\text{BG}} n_c(\mathbf{0})\mu\Delta}{M\mathcal{H}^2\mu_B}}. \quad (9)$$

Thus, on the right-hand side of the Feshbach resonance, i.e., for $B_{\text{res}} < B_0 < B_{\text{crit}} = B_{\text{res}} + \Delta$, we expect due to $a_{\text{BG}} < 0$ that the Kohn mode frequency (9) is smaller than the corresponding one without the Feshbach resonance. In the following we will show that this initial qualitative finding is confirmed by a more quantitative analysis. In particular, it will turn out that the leading change of the Kohn mode frequency far away from the Feshbach resonance is, indeed, of the order $1/\mathcal{H}^2$.

III. VARIATIONAL APPROACH

Instead of directly solving the Gross-Pitaevskii equation for the condensate wave function, it is also possible to determine its solution approximately within a variational approach [44,45]. To this end the differential equation of Gross and Pitaevskii (1) is reduced to a set of ordinary differential equations for variational parameters, which appear

in a suitable ansatz for the condensate wave function. Although this represents a tremendous simplification of the description of BEC dynamics, it has turned out to capture the essential physics. For instance, even inherent nonlinear phenomena such as parametric and geometric resonances could successively be described within this variational approach [12,13,17]. Surprisingly, for a period modulation of the s-wave scattering length around a relatively strong background value, it has turned out that the variational equations for the BEC widths coincide quantitatively even for long propagation times with the condensate widths determined from solving the GP equation [17]. Therefore, we are confident that it is suitable to work out also a variational treatment of collective excitations near a Feshbach resonance.

To this end, we start with casting Eq. (1) into a variational problem, which corresponds to the extremization of the action defined by the Lagrangian

$$L(t) = \int d\mathbf{r} \left[\frac{i\hbar}{2} \left(\psi^* \frac{\partial \psi}{\partial t} - \psi \frac{\partial \psi^*}{\partial t} \right) - \frac{\hbar^2}{2M} |\nabla \psi|^2 - V(\mathbf{r}) |\psi|^2 - \frac{g_2 N}{2} |\psi|^4 \right]. \quad (10)$$

In order to analytically study the dynamical system of a BEC with two-body contact interaction, where the dipole mode is excited in the z direction, we use a Gaussian variational ansatz which includes the center-of-mass oscillation in the z direction according to Refs. [38,44,45]. For an axially symmetric trap, this time-dependent ansatz reads

$$\psi^G(\rho,z,t) = \mathcal{N}(t) \exp \left[-\frac{\rho^2}{2u_\rho^2} + i\rho\alpha_\rho + i\rho^2\beta_\rho \right] \\ \times \exp \left[-\frac{(z-z_0)^2}{2u_z^2} + iz\alpha_z + iz^2\beta_z \right], \quad (11)$$

where $\mathcal{N} = (\pi^{3/2} u_\rho^2 u_z)^{-1/2}$ is a normalization factor, while $u_{\rho,z}$, z_0, $\alpha_{\rho,z}$, and $\beta_{\rho,z}$ denote time-dependent variational parameters, which represent radial and axial condensate widths, the center-of-mass position, and the corresponding phases. Note that the Gaussian variational ansatz (11) covers only a subset of collective excitations; for instance, it cannot describe the scissors mode [48].

Inserting the Gaussian ansatz (11) into the Lagrange function (10), we obtain

$$L(t) = -\frac{\hbar^2}{2M} \left[\frac{1}{2u_z^2} + \frac{1}{u_\rho^2} + 2u_z^2\beta_z^2 + 4z_0^2\beta_z^2 + 4z_0\beta_z\alpha_z \right. \\ \left. + \alpha_z^2 + 4u_\rho^2\beta_\rho^2 + 2\sqrt{\pi}u_\rho\beta_\rho\alpha_\rho + \alpha_\rho^2 \right] \\ - \frac{\hbar}{2} \left[u_z^2\dot{\beta}_z + 2z_0^2\dot{\beta}_z + 2z_0\dot{\alpha}_z + 2u_\rho^2\dot{\beta}_\rho + \sqrt{\pi}u_\rho\dot{\alpha}_\rho \right] \\ - V_0 - \frac{\hbar^2 N a_{BG}}{\sqrt{2\pi} M} \frac{1}{u_\rho^2 u_z} - \frac{M\omega_\rho^2}{2} \left[u_\rho^2 + \frac{\lambda^2 u_z^2}{2} + \lambda^2 z_0^2 \right] \\ + \frac{4\hbar^2 N a_{BG} \Delta}{\pi u_\rho^4 u_z^2 M} f, \quad (12)$$

where we have introduced the integral

$$f = \int_0^\infty d\rho \int_{-\infty}^\infty dz \frac{\rho \exp \left[-2\rho^2/u_\rho^2 - 2(z-z_0)^2/u_z^2 \right]}{\mathcal{H} + \frac{M\omega_\rho^2}{2\mu_B}(\rho^2 + \lambda^2 z^2)}. \quad (13)$$

From the corresponding Euler-Lagrange equations we obtain the equations of motion for all variational parameters. The phases $\alpha_{\rho,z}$ and $\beta_{\rho,z}$ can be expressed explicitly in terms of first derivatives of the widths u_ρ, u_z, and the center-of-mass coordinate z_0 according to

$$\alpha_\rho = 0, \quad \alpha_z = \frac{M}{\hbar}\dot{z}_0 - 2z_0\beta_z, \quad \beta_{\rho,z} = \frac{M}{2\hbar}\frac{\dot{u}_{\rho,z}}{u_{\rho,z}}. \quad (14)$$

Inserting Eq. (14) into the Euler-Lagrange equations for the width of the condensates u_ρ, u_z, and the center-of-mass coordinate z_0, we obtain a system of three second-order differential equations for u_ρ, u_z, and z_0: After rescaling the quantities according to

$$u_i, \rho, z, z_0 \to l(u_i, \rho, z, z_0), \quad t \to t\omega_\rho, \quad (15)$$

with the oscillating length $l = \sqrt{\hbar/(M\omega_\rho)}$, we obtain a system of second-order differential equations for u_ρ, u_z, and z_0 in the dimensionless form [38]

$$0 = \ddot{u}_\rho + u_\rho - \frac{1}{u_\rho^3} - \frac{\mathcal{P}_{BG}}{u_z u_\rho^3} \\ \times \left[1 - \frac{16\varepsilon_0 f}{\sqrt{2\pi} l^3 u_\rho^2 u_z} + \frac{4\varepsilon_0}{\sqrt{2\pi} l^2 u_\rho u_z} \frac{\partial f}{\partial u_\rho} \right], \quad (16)$$

$$0 = \ddot{u}_z + \lambda^2 u_z - \frac{1}{u_z^3} - \frac{\mathcal{P}_{BG}}{u_z^2 u_\rho^2} \\ \times \left[1 - \frac{16\varepsilon_0 f}{\sqrt{2\pi} l^3 u_\rho^2 u_z} + \frac{8\varepsilon_0}{\sqrt{2\pi} l^2 u_\rho^2} \frac{\partial f}{\partial u_z} \right], \quad (17)$$

$$0 = \ddot{z}_0 + \lambda^2 z_0 - \frac{4\mathcal{P}_{BG}\varepsilon_0}{\sqrt{2\pi} l^2 u_\rho^4 u_z^2} \frac{\partial f}{\partial z_0}. \quad (18)$$

Here we have introduced the dimensionless parameters

$$\mathcal{P}_{BG} = \sqrt{\frac{2}{\pi}} \frac{N a_{BG}}{l}, \quad \varepsilon_0 = \frac{\Delta}{\mathcal{H}}, \quad \varepsilon_1 = \frac{\mathcal{H}\mu_B}{(\hbar\omega_\rho)}, \quad \varepsilon = \varepsilon_0\varepsilon_1. \quad (19)$$

In order to study the frequencies of collective modes both in the vicinity of the Feshbach resonance and on the right-hand side of the Feshbach resonance, i.e., for $\mathcal{H} > 0$, we develop now our own approach by using the Schwinger trick [46] in order to rewrite the integral Eq. (13) in form of

$$f = l^3 \int_0^\infty d\rho \int_{-\infty}^\infty dz \int_0^\infty d\mathcal{S} \rho \exp \left[-\frac{2\rho^2}{u_\rho^2} - \frac{2(z-z_0)^2}{u_z^2} \right] \\ \times \exp \left[-\mathcal{S} - \frac{\mathcal{S}}{2\varepsilon_1}(\rho^2 + \lambda^2 z^2) \right]. \quad (20)$$

In the following, we concentrate on the topic how this violates the Kohn theorem, i.e., how the dipole-mode frequency changes when the bias magnetic field B_0 approaches the Feshbach resonance B_{res}. Within the linearization of the equations of motions (16)–(18), we have to take into the account that the equilibrium value of the center-of-mass position vanishes according to Eq. (18). This allows us to expand the integral of

Eq. (20) up to the second order of z_0, which yields

$$
\begin{aligned}
f = l^3 \int_0^\infty d\rho \int_{-\infty}^\infty dz \\
\times \int_0^\infty d\mathcal{S} \rho \left[1 + \frac{4zz_0}{u_z^2} - \frac{2z_0^2}{u_z^2} + \frac{8z^2z_0^2}{u_z^4} + \cdots \right] \\
\times \exp \left[-\frac{2\rho^2}{u_\rho^2} - \frac{2z^2}{u_z^2} - \mathcal{S} - \frac{\mathcal{S}}{2\varepsilon_1}(\rho^2 + \lambda^2 z^2) \right].
\end{aligned} \quad (21)
$$

Correspondingly, we determine the respective first derivatives $\frac{\partial f}{\partial u_\rho}$, $\frac{\partial f}{\partial u_z}$, and $\frac{\partial f}{\partial z_0}$ which appear in the equations of motion (16)–(18).

IV. RIGHT-HAND SIDE OF FESHBACH RESONANCE

We consider in this section the frequencies of collective modes when the bias field B_0 is larger than or equal to the resonant magnetic field $B_{\rm res}$, i.e., $\mathcal{H} = B_0 - B_{\rm res} \geqslant 0$.

A. Collective-mode frequencies

At first we obtain a system of three second-order ordinary differential equations for u_ρ, u_z, and z_0 in the dimensionless form after inserting Eq. (21) into Eqs. (16)–(18):

$$
\begin{aligned}
0 = \ddot{u}_\rho + u_\rho - \frac{1}{u_\rho^3} - \frac{\mathcal{P}_{\rm BG}}{u_z u_\rho^3} \\
\times \left[1 - 16 \int_0^\infty \frac{\varepsilon \varepsilon_1^{1/2} d\mathcal{S} \, e^{-\mathcal{S}} (2\varepsilon_1 + \mathcal{S}u_\rho^2)}{(4\varepsilon_1 + \mathcal{S}u_\rho^2)^2 \sqrt{4\varepsilon_1 + \mathcal{S}u_z^2\lambda^2}} + \cdots \right],
\end{aligned} \quad (22)
$$

$$
\begin{aligned}
0 = \ddot{u}_z + \lambda^2 u_z - \frac{1}{u_z^3} - \frac{\mathcal{P}_{\rm BG}}{u_z^2 u_\rho^2} \\
\times \left[1 - 16 \int_0^\infty \frac{\varepsilon \varepsilon_1^{1/2} d\mathcal{S} \, e^{-\mathcal{S}} (2\varepsilon_1 + \mathcal{S}u_z^2\lambda^2)}{(4\varepsilon_1 + \mathcal{S}u_\rho^2)(4\varepsilon_1 + \mathcal{S}u_z^2\lambda^2)^{3/2}} + \cdots \right],
\end{aligned} \quad (23)
$$

$$
\begin{aligned}
0 = \ddot{z}_0 + \lambda^2 z_0 \left[1 + \frac{16\mathcal{P}_{\rm BG}}{u_\rho^2 u_z} \right. \\
\left. \times \int_0^\infty \frac{\varepsilon \varepsilon_1^{1/2} d\mathcal{S} e^{-\mathcal{S}} \mathcal{S}}{(4\varepsilon_1 + \mathcal{S}u_\rho^2)(4\varepsilon_1 + \mathcal{S}u_z^2\lambda^2)^{3/2}} + \cdots \right].
\end{aligned} \quad (24)
$$

The time-independent solution of the condensate widths $u_\rho = u_{\rho 0}$, $u_z = u_{z0}$, and $z_0 = z_{00}$ is determined from

$$
\begin{aligned}
0 = u_{\rho 0} - \frac{1}{u_{\rho 0}^3} - \frac{\mathcal{P}_{\rm BG}}{u_{z0} u_{\rho 0}^3} \left[1 - 16\varepsilon \varepsilon_1^{1/2} \right. \\
\left. \times \int_0^\infty \frac{d\mathcal{S} e^{-\mathcal{S}}(2\varepsilon_1 + \mathcal{S}u_{\rho 0}^2)}{(4\varepsilon_1 + \mathcal{S}u_{\rho 0}^2)^2 \sqrt{4\varepsilon_1 + \mathcal{S}u_{z0}^2\lambda^2}} \right],
\end{aligned} \quad (25)
$$

$$
\begin{aligned}
0 = \lambda^2 u_{z0} - \frac{1}{u_{z0}^3} - \frac{\mathcal{P}_{\rm BG}}{u_{z0}^2 u_{\rho 0}^2} \left[1 - 16\varepsilon \varepsilon_1^{1/2} \right. \\
\left. \times \int_0^\infty \frac{d\mathcal{S} e^{-\mathcal{S}}(2\varepsilon_1 + \mathcal{S}u_{z0}^2\lambda^2)}{(4\varepsilon_1 + \mathcal{S}u_{\rho 0}^2)(4\varepsilon_1 + \mathcal{S}u_{z0}^2\lambda^2)^{3/2}} \right],
\end{aligned} \quad (26)
$$

$$
0 = z_{00}. \quad (27)
$$

Using the Gaussian approximation enables us to analytically estimate the frequencies of the low-lying collective modes [12,13,17,44,45] and the dipole-mode frequency. This is done by linearizing Eqs. (22)–(24) around the equilibrium positions (25)–(27). If we expand the condensate widths as $u_\rho = u_{\rho 0} + \delta u_\rho$, $u_z = u_{z0} + \delta u_z$, and the center-of-mass motion as $z_0 = z_{00} + \delta z_0$, insert these expressions into the corresponding equations, and expand them around the equilibrium widths by keeping only linear terms, we immediately get for the breathing and quadrupole frequencies

$$
\omega_{B,Q}^2 = \frac{\omega_\rho^2}{2} \left[m_1 + m_3 \pm \sqrt{(m_1 - m_3)^2 + 8m_2^2} \right], \quad (28)
$$

where the abbreviations m_1, m_2, and m_3 are calculated by using MATHEMATICA [49]:

$$
\begin{aligned}
m_1 = 1 + \frac{3}{u_{\rho 0}^4} + \frac{3\mathcal{P}_{\rm BG}}{u_{\rho 0}^4 u_{z0}} \left[1 - 16\varepsilon \varepsilon_1^{1/2} \right. \\
\left. \times \int_0^\infty \frac{d\mathcal{S} e^{-\mathcal{S}}(5\mathcal{S}^2 u_{\rho 0}^4 + 18\mathcal{S}u_{\rho 0}^2\varepsilon_1 + 24\varepsilon_1^2)}{3(\mathcal{S}u_{\rho 0}^2 + 4\varepsilon_1)^3 \sqrt{4\varepsilon_1 + \mathcal{S}u_{z0}^2\lambda^2}} \right],
\end{aligned} \quad (29)
$$

$$
\begin{aligned}
m_2 = \frac{\mathcal{P}_{\rm BG}}{u_{\rho 0}^3 u_{z0}^2} \left[1 - 32\varepsilon \varepsilon_1^{1/2} \right. \\
\left. \times \int_0^\infty \frac{d\mathcal{S} e^{-\mathcal{S}}(\mathcal{S}u_{\rho 0}^2 + 2\varepsilon_1)(2\varepsilon_1 + \mathcal{S}u_{z0}^2\lambda^2)}{(\mathcal{S}u_{\rho 0}^2 + 4\varepsilon_1)^2(4\varepsilon_1 + \mathcal{S}u_{z0}^2\lambda^2)^{3/2}} \right],
\end{aligned} \quad (30)
$$

$$
\begin{aligned}
m_3 = \lambda^2 + \frac{3}{u_{z0}^4} + \frac{2\mathcal{P}_{\rm BG}}{u_{\rho 0}^2 u_{z0}^3} \left[1 - 8\varepsilon \varepsilon_1^{1/2} \right. \\
\left. \times \int_0^\infty \frac{d\mathcal{S} e^{-\mathcal{S}}(16\varepsilon_1^2 + 10\mathcal{S}u_{z0}^2\varepsilon_1\lambda^2 + 3\mathcal{S}^2 u_{z0}^4\lambda^4)}{(\mathcal{S}u_{\rho 0}^2 + 4\varepsilon_1)(4\varepsilon_1 + \mathcal{S}u_{z0}^2\lambda^2)^{5/2}} \right].
\end{aligned} \quad (31)
$$

The quadrupole mode has a lower frequency and is characterized by out-of-phase radial and axial oscillations, while in-phase oscillations correspond to the breathing mode. Furthermore, the dipole-mode frequency is given by

$$
\begin{aligned}
\omega_D^2 = \lambda^2 \omega_\rho^2 \left[1 + \frac{16\mathcal{P}_{\rm BG}}{u_{\rho 0}^2 u_{z0}} \right. \\
\left. \times \int_0^\infty \frac{\varepsilon \varepsilon_1^{1/2} d\mathcal{S} \, e^{-\mathcal{S}} \mathcal{S}}{(4\varepsilon_1 + \mathcal{S}u_{\rho 0}^2)(4\varepsilon_1 + \mathcal{S}u_{z0}^2\lambda^2)^{3/2}} \right].
\end{aligned} \quad (32)
$$

B. Thomas-Fermi approximation

In order to find an analytical description for the condensate widths $u_{\rho 0}$, u_{z0}, and their ratio $u_{\rho 0}/u_{z0}$ as well as the frequencies of collective modes, we consider now the TF approximation. Thus, we neglect the respective second term in Eqs. (25) and (26), which comes from the kinetic energy. Furthermore, we use the ansatz

$$
\frac{u_{z0}\lambda}{u_{\rho 0}} = 1 + \eta \quad (33)
$$

and evaluate the resulting equations in the limit of a vanishing smallness parameter η, yielding

$$u_{\rho 0} - \frac{\mathcal{P}_{BG}}{u_{z0}u_{\rho 0}^3}\left[1 - 16\varepsilon\varepsilon_1^{1/2}\int_0^\infty d\mathcal{S}\frac{e^{-\mathcal{S}}\left(\mathcal{S}u_{\rho 0}^2 + 2\varepsilon_1\right)}{\left(\mathcal{S}u_{\rho 0}^2 + 4\varepsilon_1\right)^{5/2}}\right]$$
$$= 0, \tag{34}$$

$$\lambda^2 u_{z0} - \frac{\mathcal{P}_{BG}}{u_{z0}^2 u_{\rho 0}^2}\left[1 - 16\varepsilon\varepsilon_1^{1/2}\int_0^\infty d\mathcal{S}\frac{e^{-\mathcal{S}}\left(\mathcal{S}u_{\rho 0}^2 + 2\varepsilon_1\right)}{\left(\mathcal{S}u_{\rho 0}^2 + 4\varepsilon_1\right)^{5/2}}\right]$$
$$= 0. \tag{35}$$

Solving the remaining $\mathcal{S}$ integral we obtain the equilibrium widths $u_{\rho 0}$ and u_{z0} in TF approximation:

$$0 = u_{\rho 0}^5 - \mathcal{P}_{BG}\lambda\left[1 - \frac{\varepsilon}{3}\left(\frac{40}{u_{\rho 0}^2} + \frac{64\varepsilon_1}{u_{\rho 0}^4}\right) + \left(3u_{\rho 0}^2 + 4\varepsilon_1\right)\kappa\right], \tag{36}$$

$$\lambda u_{z0} = u_{\rho 0}, \tag{37}$$

where we have introduced the abbreviation

$$\kappa = \frac{8\varepsilon\sqrt{\pi\varepsilon_1}}{u_{\rho 0}^5}e^{4\varepsilon_1/u_{\rho 0}^2}\mathrm{Erfc}[2\sqrt{\varepsilon_1}/u_{\rho 0}], \tag{38}$$

with the complementary error function

$$\mathrm{Erfc}(x) = \frac{2}{\sqrt{\pi}}\int_x^\infty dt\,e^{-t^2}. \tag{39}$$

In the similar way we obtain the quadrupole, breathing, and dipole-mode frequencies in TF approximation by inserting Eq. (33) into Eqs. (29)–(32) and evaluating the limit $\eta \to 0$. Solving the remaining $\mathcal{S}$ integrals we obtain analytically the quadrupole and breathing frequencies in the TF approximation via Eq. (28) with the abbreviations

$$m_1 = 1 + \frac{3\mathcal{P}_{BG}\lambda}{u_{\rho 0}^5}\left[1 - \frac{8\varepsilon}{45u_{\rho 0}^7}\left(107u_{\rho 0}^5 + 408u_{\rho 0}^3\varepsilon_1\right.\right.$$
$$\left.\left. + 256u_{\rho 0}\varepsilon_1^2\right) + \frac{\kappa}{45}\left(300u_{\rho 0}^2 + 880\varepsilon_1 + \frac{512\varepsilon_1^2}{u_{\rho 0}^2}\right)\right], \tag{40}$$

$$m_2 = \frac{\mathcal{P}_{BG}\lambda^2}{u_{\rho 0}^5}\left[1 - \frac{8\varepsilon}{15u_{\rho 0}^7}\left(43u_{\rho 0}^5 + 152u_{\rho 0}^3\varepsilon_1 + 64u_{\rho 0}\varepsilon_1^2\right)\right.$$
$$\left. + \frac{\kappa}{15}\left(120u_{\rho 0}^2 + 320\varepsilon_1 + \frac{128\varepsilon_1^2}{u_{\rho 0}^2}\right)\right], \tag{41}$$

$$m_3 = \lambda^2 + \frac{2\mathcal{P}_{BG}\lambda^3}{u_{\rho 0}^5}\left[1 - \frac{16\varepsilon}{15u_{\rho 0}^7}\left(16u_{\rho 0}^5 + 64u_{\rho 0}^3\varepsilon_1\right.\right.$$
$$\left.\left. + 48u_{\rho 0}\varepsilon_1^2\right) + \frac{\kappa}{15}\left(90u_{\rho 0}^2 + 280\varepsilon_1 + \frac{192\varepsilon_1^2}{u_{\rho 0}^2}\right)\right], \tag{42}$$

whereas the dipole-mode frequency in the TF approximation reads explicitly

$$\omega_D^2 = \lambda^2\omega_\rho^2\left\{1 + \frac{32\mathcal{P}_{BG}\lambda\varepsilon}{3u_{\rho 0}^{10}}\left[u_{\rho 0}^3 + 4u_{\rho 0}\varepsilon_1\right.\right.$$
$$\left.\left. - \frac{\kappa u_{\rho 0}^5}{8\varepsilon}\times\left(3u_{\rho 0}^2 + 8\varepsilon_1\right)\right]\right\}. \tag{43}$$

C. On top of Feshbach resonance

Now, as a physically important special case, we apply the TF approximation to the condensate widths (36), (37) and to the frequencies of collective modes (28) where the abbreviations m_1, m_2, and m_3 are defined in Eqs. (40)–(43) on top of the Feshbach resonance. In the limit $\mathcal{H} \to 0$ or $\varepsilon_1 \to 0$ we obtain the condensate widths

$$u_{\rho 0}^5 - \mathcal{P}_{BG}\lambda\left(1 - \frac{40\varepsilon}{3u_{\rho 0}^2}\right) = 0, \tag{44}$$

$$\lambda u_{z0} = u_{\rho 0}, \tag{45}$$

the breathing and quadrupole frequencies (28) from

$$m_1 = 1 + \frac{3\mathcal{P}_{BG}\lambda}{u_{\rho 0}^5}\left(1 - \frac{856\varepsilon}{45u_{\rho 0}^2}\right), \tag{46}$$

$$m_2 = \frac{\mathcal{P}_{BG}\lambda^2}{u_{\rho 0}^5}\left(1 - \frac{344\varepsilon}{15u_{\rho 0}^2}\right), \tag{47}$$

$$m_3 = \lambda^2 + \frac{2\mathcal{P}_{BG}\lambda^3}{u_{\rho 0}^5}\left(1 - \frac{256\varepsilon}{15u_{\rho 0}^2}\right), \tag{48}$$

and the dipole-mode frequency

$$\omega_D^2 = \lambda^2\omega_\rho^2\left(1 + \frac{32\varepsilon\lambda\mathcal{P}_{BG}}{3u_{\rho 0}^7}\right). \tag{49}$$

All these results on top of the Feshbach resonance turn out to be finite in contrast to the finding of Ref. [38].

D. Far away from Feshbach resonance

Accordingly, we also apply the TF approximation to the condensate widths (34), (35) and to the frequencies of collective modes (28), where the abbreviations m_1, m_2, and m_3 are defined in Eqs. (40)–(43) for the case when B_0 is far away from the Feshbach resonance. In the limit $\mathcal{H} \to \infty$ or $\varepsilon_1 \to \infty$ we have to expand the complementary error function (39) for large real x

$$\mathrm{Erfc}(x) = \frac{e^{-x^2}}{\sqrt{\pi}}\left(\frac{1}{x} - \frac{1}{2x^3} + \frac{3}{4x^5} + \cdots\right), \tag{50}$$

yielding a corresponding asymptotic expansion for κ from Eq. (38)

$$\kappa = 8\varepsilon\left(\frac{1}{2u_{\rho 0}^4} - \frac{1}{16u_{\rho 0}^2\varepsilon_1} + \frac{3}{128\varepsilon_1^2} + \cdots\right). \tag{51}$$

Inserting the expansion (51) into Eqs. (36) and (40)–(43), we get for the condensate widths

$$u_{\rho 0}^5 - \mathcal{P}_{\text{BG}}\lambda \left(1 - \varepsilon_0 + \frac{u_{\rho 0}^2 \varepsilon_0}{8\varepsilon_1} + \cdots \right) = 0, \qquad (52)$$

$$\lambda u_{z0} = u_{\rho 0}, \qquad (53)$$

the breathing and quadrupole frequencies Eq. (28) are given by

$$m_1 = 1 + \frac{3\mathcal{P}_{\text{BG}}\lambda}{u_{\rho 0}^5} \left(1 - \varepsilon_0 + \frac{\varepsilon_0 u_{\rho 0}^2}{8\varepsilon_1} - \frac{17 u_{\rho 0}^4 \varepsilon_0}{192\varepsilon_1^2} + \cdots \right), \quad (54)$$

$$m_2 = \frac{\mathcal{P}_{\text{BG}}\lambda^2}{u_{\rho 0}^5} \left(1 - \varepsilon_0 - \frac{\varepsilon_0 u_{\rho 0}^2}{8\varepsilon_1} + \frac{17 u_{\rho 0}^4 \varepsilon_0}{64\varepsilon_1^2} + \cdots \right), \quad (55)$$

$$m_3 = \lambda^2 + \frac{2\mathcal{P}_{\text{BG}}\lambda^3}{u_{\rho 0}^5} \left(1 - \varepsilon_0 + \frac{\varepsilon_0 u_{\rho 0}^2}{4\varepsilon_1} - \frac{17 u_{\rho 0}^4 \varepsilon_0}{64\varepsilon_1^2} + \cdots \right), \quad (56)$$

and for the dipole frequency

$$\omega_D^2 = \lambda^2 \omega_\rho^2 \left(1 + \frac{\varepsilon_0 \mathcal{P}_{\text{BG}}\lambda}{2\varepsilon_1 u_{\rho 0}^3} + \cdots \right). \qquad (57)$$

These results for B_0 far away from the Feshbach resonance are now compared with the corresponding findings of Ref. [38], which we elaborate briefly in the next section.

E. Heuristic approximation

In this section we discuss the heuristic approximation of Ref. [38] for evaluating the integral (13). To this end we assume that the cloud size is much smaller than the oscillating amplitude, which means that the cloud experiences the same field at any point, i.e., the scattering length is homogeneous in the entire cloud. This is equivalent to stating that the numerator of the integral (13), i.e.,

$$\rho \exp\left[-2\rho^2/u_\rho^2 - 2(z - z_0)^2/u_z^2 \right] \qquad (58)$$

is much narrower than the denominator

$$\frac{1}{\mathcal{H} + \frac{M\omega_\rho^2}{2\mu_{\text{B}}}\left(\rho^2 + \lambda^2 z^2 \right)}, \qquad (59)$$

which leads to the conditions

$$u_\rho \ll \sqrt{\frac{2\mu_{\text{B}}\mathcal{H}}{M\omega_\rho^2}}, \quad u_z \ll \sqrt{\frac{2\mu_{\text{B}}\mathcal{H}}{M\omega_\rho^2\lambda^2}}. \qquad (60)$$

Thus, the heuristic approximation of Ref. [38] seems to be valid for a sufficiently large $\mathcal{H}$, i.e., far away from the Feshbach resonance.

In that case, we can expand Eq. (59) around the center of mass $\rho = 0$ and $z = z_0$, which gives us in leading order

$$\frac{1}{\mathcal{H} + \frac{M\omega_\rho^2}{2\mu_{\text{B}}}(\rho^2 + \lambda^2 z^2)} \approx \frac{1}{\mathcal{H} + \frac{M\omega_\rho^2}{2\mu_{\text{B}}}\lambda^2 z_0^2}. \qquad (61)$$

Within this approximation, the integral (13) can be evaluated exactly and yields

$$f(u_\rho, u_z, z_0) \approx \frac{\sqrt{2\pi}}{8\mathcal{H}} \frac{u_\rho^2 u_z}{\left(1 + \frac{M\omega_\rho^2 \lambda^2 z_0^2}{2\mu_{\text{B}}\mathcal{H}} \right)}. \qquad (62)$$

By substituting Eq. (62) into Eqs. (16)–(18) and after introducing dimensionless parameters according to Eq. (19) we obtain three second-order ordinary differential equations for u_ρ, u_z, and z_0 [38]. A linearization yields the frequencies of collective modes of Ref. [38] in the TF approximation to be

$$\omega_{B,Q}^2 = \omega_\rho^2 \left(2 + \frac{3}{2}\lambda^2 \pm \frac{1}{2}\sqrt{16 - 16\lambda^2 + 9\lambda^4} \right); \quad (63)$$

thus they do not depend on the bias magnetic field B_0. Correspondingly, the dipole-mode frequency of Ref. [38] in the TF approximation has the form

$$\omega_D^2 = \lambda^2 \omega_\rho^2 \left(1 + \frac{\varepsilon_0 \mathcal{P}_{\text{BG}}\lambda}{2\varepsilon_1 u_{\rho 0}^3} \right), \qquad (64)$$

where the dipole-mode frequency diverges on top of the Feshbach resonance, i.e., for $\varepsilon_1 = 0$.

V. RESULTS

We discuss in this section the respective results when the bias field B_0 is larger than or equal to the resonant magnetic field B_{res}, i.e., $\mathcal{H} = B_0 - B_{\text{res}} \geqslant 0$. To this end we follow Refs. [40,41] and consider a concrete experiment with $N = 4 \times 10^4$ atoms of a ^{85}Rb BEC in a harmonic trap with $\omega_\rho = 2\pi \times 156$ Hz along the radial direction and $\omega_z = 2\pi \times 16$ Hz along the axial direction. The Feshbach resonance parameters are given by the background value $a_{\text{BG}} = -443 a_0$, where a_0 is the Bohr radius, the width $\Delta = 10.7$ G, and the resonance location at $B_{\text{res}} = 155$ G. The magnetic dipole moment μ_{B} of ^{85}Rb [50] is equal to one Bohr magneton $m_{\text{B}} = e\hbar/(2M_e)$, which represents the magnetic moment of the Hydrogen atom with the elementary charge e and the electron mass M_e. With this the dimensionless parameters (19) have the values

$$\mathcal{P}_{\text{BG}} = -856.732, \quad \varepsilon_0\varepsilon_1 = \varepsilon = 9.6052 \times 10^4. \quad (65)$$

A. Right-hand side of Feshbach resonance

We plot in Fig. 1 the equilibrium widths of the condensate $u_{\rho 0}$, u_{z0}, and the aspect ratio of $u_{\rho 0}/u_{z0}$ as a function of magnetic field B_0 for the experimental parameters (65) with different trap anisotropy $\lambda = 0.5$ [Figs. 1(a) and 1(c)] and $\lambda = 2$ [Fig. 1(b)]. The widths of the condensate (25) and (26) are coupled, so we solve both equations iteratively. We read off that the aspect ratio $u_{\rho 0}/u_{z0}$ turns out to coincide perfectly with the trap aspect ratio λ; therefore, it is justified to use the TF approximation (33) to find an analytical understanding for the condensate widths. From Fig. 1 we also read off that the heuristic approximation of Ref. [38] is not valid on top of the Feshbach resonance and seems to be valid only far away from the Feshbach resonance. Furthermore, Fig. 1 confirms that the TF approximation in Eqs. (36) and (37) agrees quite well with the equilibrium widths determined from Eqs. (25) and (26). In addition Fig. 1(c) shows that the radial condensate
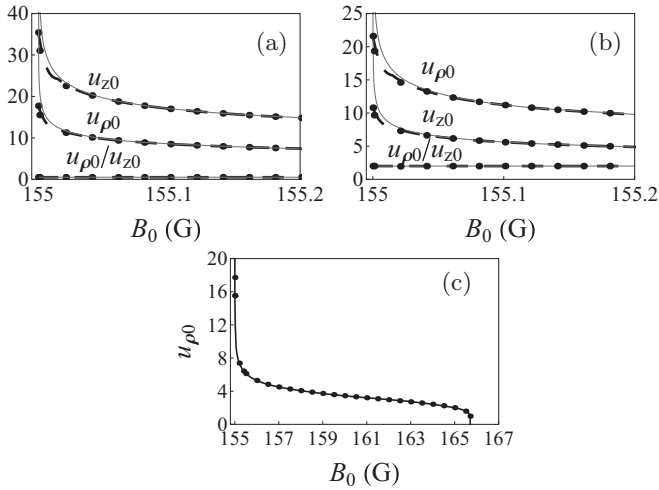
FIG. 1. Equilibrium results for dimensionless condensate widths $u_{\rho 0}$, u_{z0}, and aspect ratio $u_{\rho 0}/u_{z0}$ as a function of a magnetic field B_0 for different trap anisotropy (a), (c) $\lambda = 0.5$ and (b) $\lambda = 2$ for the experimental parameters Eq. (65). Solid, dotted, and dashed curves correspond to the heuristic approximation of Ref. [38], the exact results (25) and (26), and the TF approximation (36) and (37), respectively.

width $u_{\rho 0}$ from Eq. (25) vanishes at the critical magnetic field $B_{\rm crit} = B_{\rm res} + \Delta = 165.7$ G. As already anticipated due to the heuristic argument of Ref. [38], the system on the right-hand side of the Feshbach resonance is not stable beyond this critical magnetic field $B_{\rm crit}$.

Figures 2 and 3 show the respective frequencies of collective modes, for the experimental parameters (65) with different trap anisotropy λ. From these figures we see how the frequencies of collective modes change when one approaches the Feshbach resonance. As already expected in Eq. (9), the dipole-mode frequency on the right-hand side of the Feshbach resonance turns out to be smaller than the dipole-mode frequency far away from the Feshbach resonance. In particular we observe that the approximate solution of Ref. [38] is not valid on top of the Feshbach resonance. Our results and the approximate solution of Ref. [38] for the dipole-mode frequency in Fig. 2 disagree by only 0.05 G above the Feshbach resonance for the experimental parameters (65). However, this
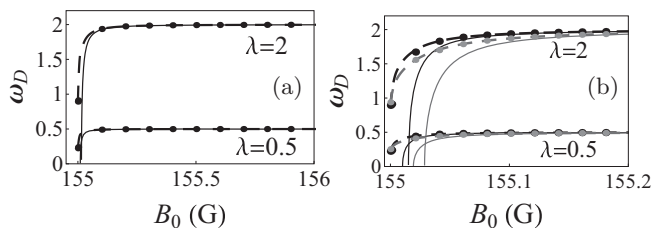

FIG. 2. Dipole-mode frequency in units of ω_ρ as a function of magnetic field B_0 for different trap anisotropy $\lambda = 0.5$ and $\lambda = 2$ (a) for the experimental parameters (65), where solid, dotted, and dashed curves correspond to the approximation solution of Ref. [38], the exact result (32), and the TF approximation (43), respectively, while panel (b) focuses on the region of interest for the experimental parameters (black) and for the hypothetical value of the Feshbach resonance $\Delta = 100.7$ G (gray) with $\lambda = 0.5$ and $\lambda = 2$.
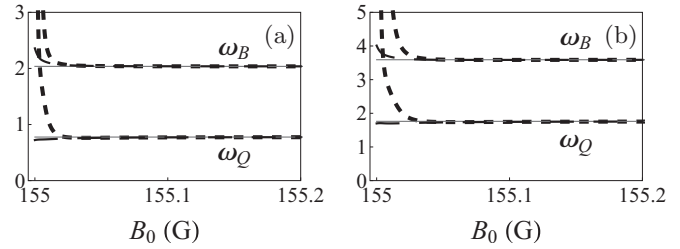

FIG. 3. Frequencies in units of ω_ρ for quadrupole mode and breathing mode as a function of a magnetic field B_0 for different trap anisotropy (a) $\lambda = 0.5$ and (b) $\lambda = 2$ for the experimental parameters (65). Solid, dashed, and square-dotted curves correspond to the approximate solution of Ref. [38], the TF approximation (28) with the abbreviations m_1, m_2, and m_3 from Eqs. (40)–(42), and the TF approximation in the limit $\mathcal{H} \to \infty$ or $\varepsilon_1 \to \infty$ (28) with the abbreviations m_1, m_2, and m_3 being defined in Eqs. (54)–(56), respectively.

is still an experimentally accessible range as the magnetic field can be controlled up to an accuracy of 1 mG [51]. Furthermore, Fig. 2(b) shows how the dipole-mode frequency changes with the bias magnetic field B_0 for a hypothetical Feshbach resonance width $\Delta = 100.7$ G. Thus, the difference between our predication and the approximate solution of Ref. [38] is more pronounced for a broader Feshbach resonance and for a pancake-like condensate.

B. On top of Feshbach resonance

We remark that approaching the Feshbach resonance and performing the TF limit represent commuting procedures within our theory. In contrast to our findings the heuristic approximation of Ref. [38] fails to predict a finite value for the dipole-mode frequency on top of the Feshbach resonance [52].

Figure 4 shows the equilibrium widths of the condensate $u_{\rho 0}$, u_{z0} and the aspect ratio $u_{\rho 0}/u_{z0}$ following from the exact results of Ref. [52] as solid lines versus trap aspect ratio λ and the experimental parameters (65). From Fig. 4(b) we read off that the aspect ratio $u_{\rho 0}/u_{z0}$ turns out to coincide perfectly with the trap aspect ratio λ.

In Fig. 5(a) we plot the dipole-mode frequency as a function trap anisotropy λ. The solid black curve corresponds to the dipole-mode frequency far away from the Feshbach resonance $\omega_D = \lambda$. Furthermore, the solid gray curve corresponds to
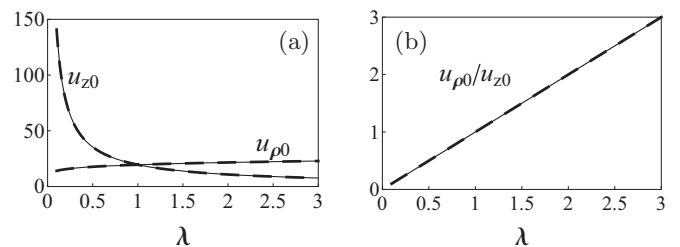

FIG. 4. Equilibrium results for (a) dimensionless condensate widths $u_{\rho 0}$, u_{z0} and (b) aspect ratio $u_{\rho 0}/u_{z0}$ as a function of trap aspect ratio λ for the experimental parameters (65). Solid and dashed curves correspond to the exact results of Ref. [52] and the TF approximation (44) and (45), respectively.
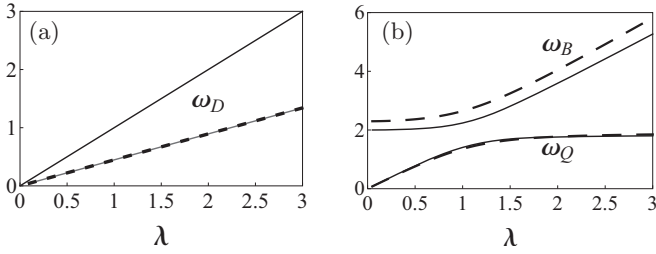
FIG. 5. Frequencies in units of ω_ρ for (a) dipole mode and (b) breathing mode and quadrupole mode as a function of trap aspect ratio λ for the experimental parameters (65). (a) The solid black curve corresponds to the dipole-mode frequency far away the Feshbach resonance which means that $\omega_D = \lambda \omega_\rho$. The solid gray and dashed curves correspond to the exact result of Ref. [52] and in the TF approximation (49), respectively. (b) The solid and dashed curves correspond to Eqs. (63) and in the TF approximation (28), respectively, where the abbreviations are defined in Eqs. (46)–(48).

the exact result of dipole-mode frequency on top of the Feshbach resonance [52] and the dashed curve corresponds to the dipole-mode in the TF approximation (49) for the experimental parameters (65). This result could be seen as being inconsistent with the Kohn theorem [21], which says that the dipole frequency is equal to the trap frequency and does not depend on the two-body interaction strength. However, the result of the Kohn theorem is a consequence of the translational invariance of the two-body interaction, which is no longer true in our case due to Eq. (5). As a consequence, the dipole-mode frequency in the exact result of Ref. [52] and its TF approximation (49) depend on the two-body interaction strength $\mathcal{P}_{BG}$ and the anisotropy of the confining potential λ both explicitly and implicitly via the equilibrium values of the condensate widths from Ref. [52].

In Fig. 5(b) we also show the breathing and quadrupole-mode frequencies as a function of trap anisotropy λ. The solid curves correspond to the frequencies of collective modes far away from the Feshbach resonance, i.e., for $\varepsilon = 0$, while the dashed curves correspond to the frequencies of collective modes on top of the Feshbach resonance and in the TF approximation (28), with abbreviations m_1, m_2, and m_3 defined in Eqs. (46)–(48) for the experimental parameters Eq. (65). We observe that approaching the Feshbach resonance leads to a significant change of the breathing-mode frequency, whereas the quadrupole-mode frequency remains basically unaffected.

C. Far away from Feshbach resonance

As we have $\varepsilon_0 \to 1/\mathcal{H}$ and $\varepsilon_1 \to \mathcal{H}$ according to Eq. (19), the results (52)–(57) represent the $1/\mathcal{H}$ and $1/\mathcal{H}^2$ corrections for the respective quantities. At first we observe by comparing Eqs. (52) and (53) that the heuristic approximation of Ref. [38] reproduces correctly the $1/\mathcal{H}$ correction for the condensate widths but fails to determine the subsequent $1/\mathcal{H}^2$ correction. This is not surprising because the heuristic approximation (62) of Ref. [38] for the integral (13) is only exact up to order $1/\mathcal{H}$. But we read off from our results in Eq. (57) for the dipole-mode frequency that the leading-order correction to the Kohn theorem near Feshbach resonance is in fact of the

order $1/\mathcal{H}^2$. Therefore, the corresponding predication of the heuristic approximation of Ref. [38] is even incorrect far away from the Feshbach resonance.

In addition, the similar situation for the breathing and quadrupole frequencies shows that the leading order of our results (28), with the abbreviations m_1, m_2, and m_3 from Eqs. (54)–(56), presented in Fig. 3, is $1/\mathcal{H}^2$ and that the frequencies depend strongly on the magnetic field B_0 and are divergent on top of the Feshbach resonance, while the frequencies of the heuristic approximation of Ref. [38] fail to determine the correct $1/\mathcal{H}^2$ correction and depend only on the trap anisotropy λ, i.e., they do not depend on the bias magnetic field B_0.

VI. CONCLUSIONS

We have studied in detail how the dipole-mode frequency and the collective excitation modes of a harmonically trapped Bose-Einstein condensate plus a bias potential change on the right-hand side and on top of the Feshbach resonance. To this end, we have derived equations of motion (16)–(18) for the variational parameters which describe the radial and axial condensate widths as well as the center-of-mass position and have shown how to extract the frequencies of the low-lying collective modes. At first we analyzed our own treatment which is based on rewriting the integral in Eq. (20) with the help of the Schwinger trick [46]. Then we studied the consequences of this integral representation for the collective-mode frequencies both on the right-hand side and on top of the Feshbach resonance.

On the right-hand side of the Feshbach resonance we found that the system is not stable beyond the critical magnetic field B_{crit}. Furthermore, we have shown how the frequencies of the collective modes change when one approaches the Feshbach resonance. As expected initially, the dipole-mode frequency for the exact result and the TF approximation on the right-hand side of the Feshbach resonance turn out to be smaller than the dipole-mode far away from the Feshbach resonance. Furthermore, we discussed the TF approximation for the condensate widths and the frequencies of collective modes in two limits. At first we considered the limit on top of the Feshbach resonance, i.e., $\mathcal{H} \to 0$ or $\varepsilon_1 \to 0$ and, afterwards, we discussed the limit far away from the Feshbach resonance, i.e., $\mathcal{H} \to \infty$ or $\varepsilon_1 \to \infty$.

Our results and the approximate solution of Ref. [38] disagree for only about 0.05 G above the Feshbach resonance for the experimental parameters of Refs. [40,41], but this is still large enough to be experimentally accessible because the magnetic field can be tuned up to 1 mG [51]. Thus, the presented results for the violation of the Kohn theorem could, in principle, be detected in future experiments.

Furthermore, our improvement of the variational calculation of Ref. [38] suggests the principle question to which extent and with which accuracy the Gaussian ansatz (11) is really valid. To this end it would be necessary to solve the underlying Gross-Pitaevskii equation numerically with the same parameters and to compare the results in detail with the variational calculation. Such an initial comparison has already been performed in Ref. [38] by following Ref. [53] (see also Ref. [54]), yielding a preliminary validation of the

variational approach even in the immediate vicinity of the Feshbach resonance.

Finally, we remind the reader that the Gross-Pitaevskii equation is only valid within a mean-field description for a dilute Bose gas with a weak two-particle interaction. Once strong interactions occur near a Feshbach resonance, this mean-field picture breaks down and quantum fluctuations have to be taken into account. Following Refs. [55,56] this yields additional terms in the variational equations of motion whose impact upon the violation of the Kohn theorem would be interesting to study. For very strong interaction strengths there are even indications that the condensate wave function follows from a generalization of the Gross-Pitaevskii equation where both time and space derivatives turn out to be fractional [57].

[1] D. M. Stamper-Kurn, H. J. Miesner, S. Inouye, M. R. Andrews, and W. Ketterle, Phys. Rev. Lett. **81**, 500 (1998).

[2] D. S. Jin, J. R. Ensher, M. R. Matthews, C. E. Wieman, and E. A. Cornell, Phys. Rev. Lett. **77**, 420 (1996).

[3] M.-O. Mewes, M. R. Andrews, N. J. van Druten, D. M. Kurn, D. S. Durfee, C. G. Townsend, and W. Ketterle, Phys. Rev. Lett. **77**, 988 (1996).

[4] Y. Castin and R. Dum, Phys. Rev. Lett. **77**, 5315 (1996).

[5] F. Dalfovo, C. Minniti, and L. P. Pitaevskii, Phys. Rev. A **56**, 4855 (1997).

[6] J. J. García-Ripoll, V. M. Pérez-García, and P. Torres, Phys. Rev. Lett. **83**, 1715 (1999).

[7] J. J. G. Ripoll and V. M. Pérez-García, Phys. Rev. A **59**, 2220 (1999).

[8] A. I. Nicolin, Phys. Rev. E **84**, 056202 (2011).

[9] G. Hechenblaikner, O. M. Maragò, E. Hodby, J. Arlt, S. Hopkins, and C. J. Foot, Phys. Rev. Lett. **85**, 692 (2000).

[10] E. Hodby, O. M. Maragò, G. Hechenblaikner, and C. J. Foot, Phys. Rev. Lett. **86**, 2196 (2001).

[11] Y. Zhou, W. Wen, and G. Huang, Phys Rev B **77**, 104527 (2008).

[12] I. Vidanović, H. Al-Jibbouri, A. Balaž, and A. Pelster, Phys. Scr., T **149**, 014003 (2012).

[13] H. Al-Jibbouri, I. Vidanović, A. Balaž, and A. Pelster, J. Phys. B **46**, 065303 (2013).

[14] E. R. F. Ramos, E. A. L. Henn, J. A. Seman, M. A. Caracanhas, K. M. F. Magalhães, K. Helmerson, V. I. Yukalov, and V. S. Bagnato, Phys. Rev. A **78**, 063412 (2008).

[15] S. E. Pollack, D. Dries, M. Junker, Y. P. Chen, T. A. Corcovilos, and R. G. Hulet, Phys. Rev. Lett. **102**, 090402 (2009).

[16] S. E. Pollack, D. Dries, R. G. Hulet, K. M. F. Magalhães, E. A. L. Henn, E. R. F. Ramos, M. A. Caracanhas, and V. S. Bagnato, Phys. Rev. A **81**, 053627 (2010).

[17] I. Vidanović, A. Balaž, H. Al-Jibbouri, and A. Pelster, Phys. Rev. A **84**, 013618 (2011).

[18] S. Sabari, R. V. J. Raja, K. Porsezian, and P. Muruganandam, J. Phys. B: At., Mol. Opt. Phys. **43**, 125302 (2010).

[19] A. I. Nicolin, Rom. Rep. Phys. **63**, 1329 (2011).

[20] W. Cairncross and A. Pelster, arXiv:1209.3148.

[21] W. Kohn, Phys. Rev. **123**, 1242 (1961).

[22] A. L. Fetter and D. Rokhsar, Phys. Rev. A **57**, 1191 (1998).

[23] E. Zaremba, T. Nikuni, and A. Griffin, J. Low Temp. Phys. **116**, 277 (1999).

[24] M. J. Bijlsma and H. T. C. Stoof, Phys. Rev. A **60**, 3973 (1999).

[25] A. Minguzzi and M. P. Tosi, J. Phys.: Condens. Matter **9**, 10211 (1997).

[26] J. Reidl, G. Bene, R. Graham, and P. Szépfalusy, Phys. Rev. A **63**, 043605 (2001).

[27] A. Minguzzi, Phys. Rev. A **64**, 033604 (2001).

[28] T. Maruyama and G. F. Bertsch, Phys. Rev. A **77**, 063611 (2008).

[29] A. Banerjee, J. Phys. B **42**, 235301 (2009).

[30] J.-Y. Zhang, S.-C. Ji, Z. Chen, L. Zhang, Z.-D. Du, B. Yan, G.-S. Pan, B. Zhao, Y.-J. Deng, H. Zhai, S. Chen, and J.-W. Pan, Phys. Rev. Lett. **109**, 115301 (2012).

[31] Y. Li, G. I. Martone, and S. Stringari, Euro. Phys. Lett. **99**, 56008 (2012).

[32] F. Ferlaino, R. J. Brecha, P. Hannaford, F. Riboli, G. Roati, G. Modugno, and M. Inguscio, J. Opt. B **5**, S3 (2003).

[33] S. Chiacchiera, T. Macrì, and A. Trombettoni, Phys. Rev. A **81**, 033624 (2010).

[34] Y. Lu, W. Xiao-Rui, L. Ke, T. Xin-Zhou, X. Hong-Wei, and L. Bao-Long, Chin. Phys. Lett. **26**, 076701 (2009).

[35] C. J. Pethick and H. Smith, *Bose-Einstein Condensation in Dilute Gases*, 2nd ed. (Cambridge University Press, Cambridge, 2008).

[36] S. Stringari, Phys. Rev. Lett. **77**, 2360 (1996).

[37] H. Ott, J. Fortágh, S. Kraft, A. Günther, D. Komma, and C. Zimmermann, Phys. Rev. Lett. **91**, 040402 (2003).

[38] E. R. F. Ramos, F. E. A. dos Santos, M. A. Caracanhas, and V. S. Bagnato, Phys. Rev. A **85**, 033608 (2012).

[39] T. Esslinger, I. Bloch, and T. W. Hänsch, Phys. Rev. A **58**, R2664 (1998).

[40] P. A. Altin, N. P. Robins, D. Döring, J. E. Debs, R. Poldy, C. Figl, and J. D. Close, Rev. Sci. Instrum. **81**, 063103 (2010).

[41] C. Chin, R. Grimm, P. Julienne, and E. Tiesinga, Rev. Mod. Phys. **82**, 1225 (2010).

[42] E. P. Gross, Nuovo Cimento **20**, 454 (1961).

[43] L. P. Pitaevskii, Sov. Phys. JETP **13**, 451 (1961).

[44] V. M. Pérez-García, H. Michinel, J. I. Cirac, M. Lewenstein, and P. Zoller, Phys. Rev. Lett. **77**, 5320 (1996).

[45] V. M. Pérez-García, H. Michinel, J. I. Cirac, M. Lewenstein, and P. Zoller, Phys. Rev. A **56**, 1424 (1997).

[46] H. Kleinert and V. Schulte-Frohlinde, *Critical Properties of Φ^4-Theories* (World Scientific, Singapore, 2001).

[47] A. J. Moerdijk, B. J. Verhaar, and A. Axelsson, Phys. Rev. A **51**, 4852 (1995).

[48] D. Guéry-Odelin and S. Stringari, Phys. Rev. Lett. **83**, 4452 (1999).

[49] *Mathematica* symbolic calculation software package, http://www.wolfram.com/mathematica

[50] S. Yi and L. You, Phys. Rev. A **67**, 045601 (2003).

[51] B. Pasquiou, E. Maréchal, G. Bismut, P. Pedri, L. Vernac, O. Gorceix, and B. Laburthe-Tolra, Phys. Rev. Lett. **106**, 255303 (2011).

[52] H. Al-Jibbouri, Ph.D. thesis, Free University of Berlin, in preparation.

[53] P. Muruganandama and S. K. Adhikari, Comput. Phys. Commun. **180**, 1888 (2009).

[54] D. Vudragovic, I. Vidanovic, A. Balaz, P. Muruganandam, and S. K. Adhikari, Comput. Phys. Commun. **183**, 2021 (2012).

[55] A. R. P. Lima and A. Pelster, Phys. Rev. A **84**, 041604 (2011).

[56] A. R. P. Lima and A. Pelster, Phys. Rev. A **86**, 063609 (2012).

[57] H. Kleinert, Europhys. Lett. **100**, 10001 (2012).